Supporting Information

Assembling 1D double-shell PPy@Air@MnO_2 nanotube with enhanced microwave absorption performance

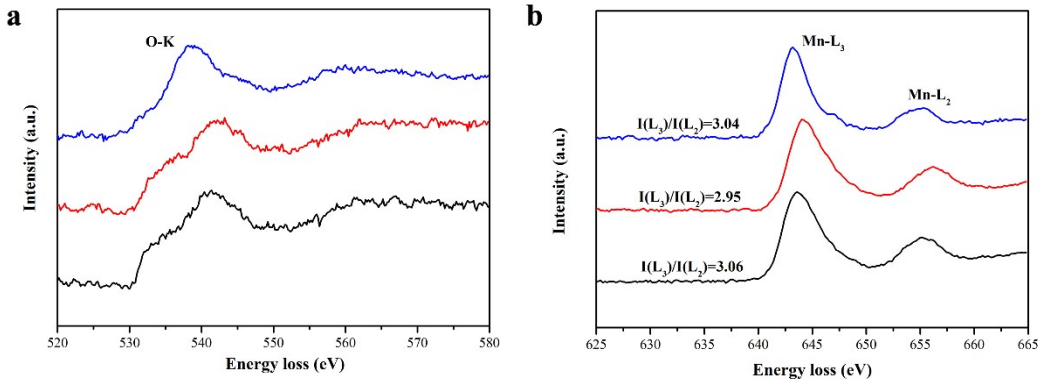

Figure S1 EELS characterization of MnO_2 nanosheets. (a) O-K spectra and (b) Mn-$L_{2,3}$ EEL spectra acquired from the MnO_2 nanosheets. Conventionally, the intersity ratios $I(L_3)/I(L_2)$ of Mn-$L_{2,3}$ edges can detect the valence of Mn quantitatively. As shown in Figure S1b, the valence of Mn is detemined to be +4, demonstrating the formation of MnO_2 nanosheets.

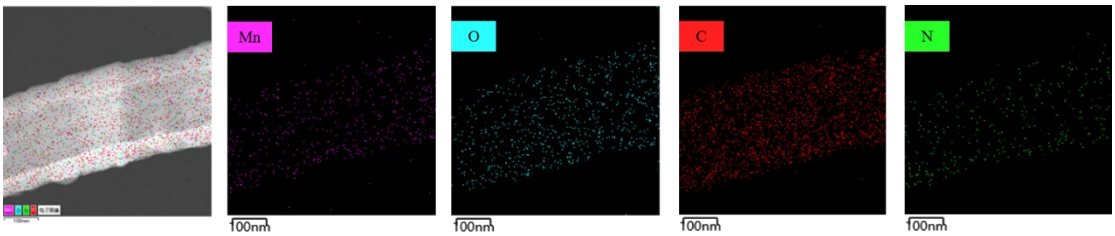

Figure S2. EDS mapping of O, Mn, N and C inside HPM-1 sample.

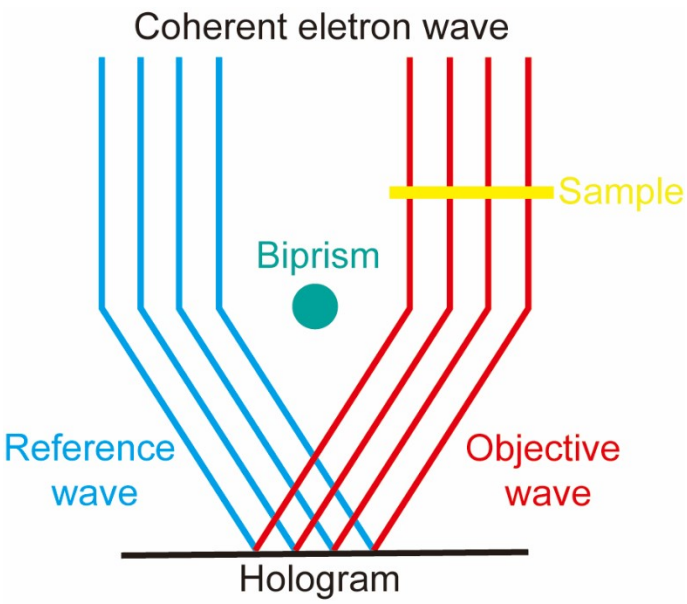

Figure S3. The optical principle of electron holography in TEM.
Electron holography in TEM is a powerful technique to measure the electrostatic potential distribution within materials. In the principle of holography, the potential field, electric field, and magnetic field in the sample unavoidably trigger the phase changes of the electron wave (objective wave), which passes through the specimen. Other electron waves passing through the vacuum act as the reference wave. A biprism below the objective lens was employed to deflect the objective wave and the reference wave to generate holograms, which can be used to calculate the phase disturbance. Based on the phase disturbance, the electric field and corresponding charge distribution can be directly determined by simply taking the divergence operation.

Table S1. MA performance of the related absorbents in previous references and this work

Absorbents	Thickness [mm]	RL_{Max} [dB]	EAB[GHz]	Refs
α-MnO_2	1.9	−41	8.7	S1
PDA@α-MnO_2	3.0	−21.8	3.28	S2
CC@δ-MnO_2	2.0	−25.3	-	S3
PPy@PANI	2.0	−34.8	4.7	S4
Fe_3O_4@ PPy	2.0	−41.6	4.2	S5
MnO_2/PANI	2.0	−20.9	4.2	S6
Fe_3O_4@δ-MnO_2	4.0	−42.6	4.1	S7
MnO_2@$NiMoO_4$	3.0	−31.4	4.5	S8
PPy@MnO_2	2.94	−52.49	3.84	This work

References

S1. M. Zhou, X. Zhang, J. M. Wei, S. L. Zhao, L. Wang and B. X. Feng, *J. Phys. Chem., C*, 2011, **115**, 1398-1402.

S2. W. She, H. Bi, Z. W. Wen, Q. H. Liu, X. B. Zhao, J. Zhang and R. C. Che, *ACS appl. Mater. Interfaces*, 2016, **8**, 9782-9789.

S3. X. Li, L. Wang, W. You, L. Xing, L. Yang, X. Yu, J. Zhang, Y. Li and R. Che, *Nanoscale*, 2019, **11**, 13269-13281.

S4. C. H. Tian, Y. C. Du, P. Xu, R. Qiang, Y. Wang, D. Ding, J. L. Xue, J. Ma, H. T. Zhao and X. J. Han, *ACS appl. Mater. Interfaces*, 2015, **7**, 20090-20099.

S5. Z. C. Wu, D. G. Tan, K. Tian, W. Hu, J. J. Wang, M. X. Su and L. Li, *J. Phys. Chem. C*, 2017, **121**, 15784-15792.

S6. J. Hu, Y. Duan, J. Zhang, H. Jing, S. Liu and W. Li, *Physica B-Condensed Matter*, 2011, **406**, 1950-1955.

S7. M. T. Qiao, X. F. Lei, Y. Ma, L. D. Tian, W. B. Wang, K. H. Su and Q. Y. Zhang, *J. Alloy. Compd.*, 2017, **693**, 432-439.

S8. X. X. Wang, B. Q. Zhang, M. X. Yu and J. Q. Liu, *Rsc Adv.*, 2016, **6**, 36484-36490.